ASSEMBLY OF THE GLOMERULAR FILTRATION SURFACE

Differentiation of Anionic Sites in Glomerular Capillaries of Newborn Rat Kidney

WESTLEY H. REEVES, YASHPAL S. KANWAR, and MARILYN GIST FARQUHAR

From the Section of Cell Biology, Yale University School of Medicine, 333 Cedar Street, New Haven, Connecticut 06510

ABSTRACT

Glomerular development was studied in the newborn rat kidney by electron microscopy and cytochemistry. Glomerular structure at different developmental stages was related to the permeability properties of its components and to the differentiation of anionic sites in the glomerular basement membrane (GBM) and on endothelial and epithelial cell surfaces. Cationic probes (cationized ferritin, ruthenium red, colloidal iron) were used to determine the time of appearance and distribution of anionic sites, and digestion with specific enzymes (neuraminidase, heparinase, chondroitinases, hyaluronidases) was used to determine their nature. Native (anionic) ferritin was used to investigate glomerular permeability. The main findings were: (*a*) The first endothelial fenestrae (which appear before the GBM is fully assembled) possess transient, negatively charged diaphragms that bind cationized ferritin and are impermeable to native ferritin. (*b*) Two types of glycosaminoglycan particles can be identified by staining with ruthenium red. Large (30-nm) granules are seen only in the cleft of the S-shaped body at the time of mesenchymal migration into the renal vesicle. They consist of hyaluronic acid and possibly also chondroitin sulfate. Smaller (10–15-nm) particles are seen in the earliest endothelial and epithelial basement membranes (S-shaped body stage), become concentrated in the laminae rarae after fusion of these two membranes to form the GBM, and contain heparan sulfate. They are assumed to be precursors of the heparan sulfate–rich granules present in the mature GBM. (*c*) Distinctive sialic acid–rich, and sialic acid–poor plasmalemmal domains have been delineated on both the epithelial and endothelial cell surfaces. (*d*) The appearance of sialoglycoproteins on the epithelial cell surface coincides with the development of foot processes and filtration slits. (*e*) Initially the GBM is loosely organized and quite permeable to native ferritin; it becomes increasingly impermeable to ferritin as the lamina densa becomes more compact. (*f*) The number of endothelial fenestrae and open epithelial slits increases as the GBM matures and becomes organized into an effective barrier to the passage of native ferritin.

During filtration, the glomerular capillary wall functions as both a size-selective and a charge-selective barrier to the passage of macromolecules (5, 6). The evidence available at present (as reviewed in reference 13) indicates that the glomerular basement membrane (GBM) functions both as the main size-selective (7, 14) and charge-selective (32) barrier of the glomerulus because normally neutral or anionic macromolecules fail to penetrate beyond the lamina rara interna of the GBM. Clearly, however, the organization of the adjacent cellular layers can affect filtration behavior. In particular, the numbers of both endothelial fenestrae and epithelial slits would be expected to modify hydraulic fluxes across the glomerulus (12), and the number and distribution of fixed, negatively charged sites in the GBM (8, 20, 32) and on the epithelial and endothelial cell surfaces (19, 29, 30) might also be expected to modify the behavior of the filter. It has proved to be difficult to investigate the modulating effects of the cellular layers on filtration behavior in the normal, mature kidney. The newborn rat kidney represents an unusually favorable situation for examining the interplay between the organization of glomerular capillaries and the filtration function of the glomerulus, because, in the newborn rat, renal function commences but the kidney is still immature—glomeruli are still differentiating and all stages in development (from the early embryonic precursors to mature, functional glomeruli) are present in a single kidney. Therefore, this provides the opportunity to study the differentiation of the glomerular filtration surface from a situation in which the GBM is loosely organized (31, 45, 46) and is backed on either side by continuous endothelial and epithelial layers (lacking fenestrae, foot processes, and concentrations of negatively charged sites) to the well-known mature arrangement. In this study, we have investigated the sequential steps involved in the assembly of the glomerular filtration surface in the newborn rat kidney; we have paid particular attention to the time of appearance, distribution, and nature of anionic sites in the various layers. In addition, we have studied the functional properties of the immature glomerulus by determining the permeability of its layers to native ferritin.

MATERIALS AND METHODS

Materials

For these studies, we used 74 2- to 5-d-old Charles River CD rats weighing 8–14 g. Horse-spleen ferritin (twice crystallized, cadmium free) was obtained from Calbiochem-Behring Corp., San Diego, Calif.; ruthenium red, from Ventron Corp., Danvers, Mass.; neuraminidase (*Clostridium perfringens*, NEUA), from Worthington Biochemical Co., Freehold, N. J.; bovine testicular hyaluronidase (type VI), and chondroitin sulfates (types A, B, and C) and hyaluronic acid (grade I), from Sigma Chemical Co., St. Louis, Mo.; chondroitinase ABC (*Proteus vulgaris*), chondroitinase AC, and streptomyces hyaluronidase, from Miles Laboratories, Elkhart, Ind.; and leech hyaluronidase, from Biotrics, Inc., Boston, Mass. Heparan sulfate was obtained from Dr. Martin Mathews. Cationized ferritin (pI 7.3) was prepared by the methods of Rinehart and Abul-Haj (33). Enzymes were tested for proteolytic activity by the Azocoll assay (28) and found to be free of proteolytic activity.

Kidney Perfusion

Each rat was anesthetized with ether, and the kidneys were perfused through the left ventricle as follows: after the kidneys and inferior vena cava were exposed, the thorax was opened by right and left paramedian incisions; the thorax was retracted superiorly, and a 28-gauge needle, connected by polyethylene tubing to the syringe containing the perfusate, was inserted into the left ventricle. The inferior vena cava was nicked below the level of the renal vein and perfusion at a rate of 1.0 ml/min was begun, first with normal saline (to wash out the blood), then with fixative or other solutions as described below. The fixed kidneys were removed and cut into slices (0.5 mm^3) using a razor blade, or sectioned (at 40 μm) using a Smith-Farquhar (TC-2) tissue sectioner (DuPont Instruments-Sorvall, DuPont Co., Newtown, Conn.).

Staining with Cationic Probes

Three different cationic probes were used, but the method of application varied with each probe as described below.

CATIONIZED FERRITIN (CF): CF of narrow range (pI 7.3) was suspended in normal saline (50 mg/ml) and injected into the inferior vena cava (0.05 ml/10 g body weight) over a period of 1–2 mm. After 5–10 min, the kidney was perfused (via the left ventricle as described above) with 10 ml of normal saline, then with 1 ml of 0.1 M KCl (to remove nonspecific binding [20]), and finally with 5–10 ml of Karnovsky's fixative (1% formaldehyde and 3% glutaraldehyde in 0.1 M cacodylate buffer, pH 7.4, with 4.4 mM $CaCl_2$). Slices (0.25–0.50 mm) were prepared and fixed for an additional 90 min in the same fixative before postfixation in OsO_4.

RUTHENIUM RED (RR): The general method of Luft (27) was used. In some cases, kidneys were flushed with saline, then perfused sequentially with 1% formaldehyde in 0.1 M cacodylate buffer (5 ml over 3–5 min) and Karnovsky's fixative containing 0.2% RR (10 ml over 10 min). Slices were prepared and fixed for an additional 3 h in the same mixture, placed in 0.1% RR in 0.1 M cacodylate buffer overnight, and postfixed in OsO_4 containing 0.05% RR for 3 h. In other cases, kidneys were fixed (by perfusion with Karnovsky's fixative), and 40-μm chopper sections were prepared and stained in 0.05% RR for 3 h.

COLLOIDAL IRON (CI): Kidneys were fixed by perfusion with Karnovsky's fixative and cut into wedges, which were immersed in the same fixative for 90 min. 40-μm Sections were prepared and floated for 90 min in CI staining solution (4 parts CI stock to 1 part glacial acetic acid, pH 1.6) and rinsed with 12% acetic acid and distilled water before postfixation in OsO_4.

Injection of Native Ferritin (NF)

Horse-spleen ferritin (100 mg/ml in normal saline) was given to anesthetized animals by injection into the inferior vena cava

(0.05 ml/10 g body weight). After 10 min, the kidneys were fixed *in situ* by injection of Karnovsky's fixative into the renal parenchyma as previously described (7). Kidney slices were then prepared and either postfixed for 2 h in OsO_4 or treated with ferrocyanide-reduced OsO_4 (24).

Enzyme Digestion Studies

Kidney tissue was briefly fixed by perfusion and flushed with saline. 40-μm Sections were prepared and incubated with various enzyme solutions, after which they were stained with CI or RR. CI staining was used primarily to evaluate removal of anionic sites from cell surfaces, whereas RR was used primarily to investigate effects of enzymes on proteoglycan granules. The fixation and incubation conditions (taken from the work of others) varied in the two cases. Tissues to be stained with CI were perfused for 5–10 min with Karnovsky's fixative, followed by immersion in the same fixative for 15 min. Sections were incubated in either neuraminidase (0.5 U/ml) (23) or in bovine testicular hyaluronidase (6,000 U/ml) in 0.1 M NaCl-acetate buffer, pH 5.4, for 8 h at 37°C (48). For tissue to be stained with RR, fixation was limited to brief (5-min) perfusion with Karnovsky's fixative or 5% formalin. Sections were incubated for 12 h at 37°C in leech hyaluronidase (0.5 mg/ml) or streptomyces hyaluronidase (100 U/ml) in citrate-phosphate buffer, pH 5.6 (35), or in chondroitinase ABC or chondroitinase AC (2.5 U/ml) in 0.1 M Tris-HCl buffer containing 0.1 M NaCl, pH 8.0 (48).[1]

Controls consisted of sections incubated under identical conditions in buffer without enzyme.

Characterization of Enzymes

The qualitative activity of the enzymes against glycosaminoglycan GAG standards was determined as follows: 5-μl aliquots of enzyme (leech hyaluronidase, 1 mg/ml; chondroitinase ABC and chondroitinase AC, 5 U/ml; streptomyces hyaluronidase, 200 U/ml) were incubated for 4 h with 20 μl of the following GAG: chondroitin A, B, or C, heparan sulfate, or hyaluronic acid, each at a concentration of 1 mg/ml.

Cellulose acetate paper was soaked in barium acetate, blotted with filter paper, and 5 μl of each of the enzyme-GAG mixtures and 2.5 μl of each of the undigested GAG standards were spotted on the paper in rows. The spots were stained with 0.1% alcian blue in 0.1% acetic acid for 1 min and decolorized with 10% acetic acid. Chondroitinase ABC was found to digest chondroitins 4- and 6-sulfates, dermatan sulfate, and hyaluronic acid; chondroitinase AC digested chondroitins 4- and 6-sulfates and hyaluronic acid, and leech and streptomyces hyaluronidases digested only hyaluronic acid (see Table I).

Tissue Processing

After postfixation with OsO_4, kidney tissues (both slices and sections) were dehydrated in ethanol and propylene oxide and embedded in Epon. Thick sections (0.5 μm) were prepared and stained with azure II–methylene blue. Glomeruli were selected by trimming the block so as to leave only the subcapsular region (containing immature glomeruli) and trimming away the corticomedullary region (containing more mature glomeruli).

Thin sections (50 nm) were prepared, placed on carbon-coated grids, and stained with uranyl acetate, lead citrate, or bismuth (1) before examination in a Siemens Elmiskop 101 or a Philips 301 electron microscope operating at 80 kV.

RESULTS

General Description of Glomerular Development

The rat kidney is immature at birth, and glomeruli continue to differentiate up to 2 wk postpartum (11). Accordingly, all stages of development can be studied in a single kidney, the least mature glomeruli being located nearest the renal capsule and the most mature nearest the medulla. We have previously defined four stages of glomerular development (31; diagrammed in Fig. 1), which are convenient for describing the differentiation of glomerular components. Briefly, the main events in glomerular differentiation of interest in this study are as follows: During the vesicle stage, the glomerulus consists of an undifferentiated cluster of cells. During the S-shaped body stage, it becomes organized into a layer of columnar epithelial cells joined by extensive occluding junctions with a rudimentary basement membrane (Fig. 2) at their base and a continuous endothelial cell layer also with a rudimentary basement membrane. During the capillary loop stage, endothelial and mesangial cells differentiate, foot processes and endothelial fenestrae appear, the two rudimentary basement membranes (epithelial and endothelial) fuse, and the GBM becomes organized into its characteristic layers. The final differentiation of the glomerular components to their adult arrangement (with filtration slits and attenuated endothelium) is completed during the maturing stage.

Development of Glomerular Components

ENDOTHELIUM: The earliest endothelial cells are cuboidal, lack fenestrae (Fig. 3), and occupy the cleft of the S-shaped body. Early in the capillary loop stage, these cells proliferate, flatten, rearrange to form the lining of capillary lumina, and develop fenestrae. The earliest fenestrae are closed by thin diaphragms (Fig. 4), but later (toward the middle of this stage) the diaphragms disappear, the endothelium becomes progressively more attenuated, and increasing numbers of open fenestrae are seen (Figs. 5 and 6).

[1] The conditions for enzyme incubations (enzyme concentration, pH, and buffers) followed closely those used previously on isolated GBM (21) or GAG isolated from GBM (22) except that the incubation times were increased from 60 min to up to 12 h. This was necessary because the sections used in the present work were prefixed (see also reference 48).

TABLE I

Effects of Enzyme Treatments on Staining of Anionic Sites in the Developing Glomerulus

	Substrate specificity	30-nm Granules	GBM (10–15-nm) Granules	Epithelial surface	Endothelial surface
RUTHENIUM RED STAINING					
Buffer controls		+‡	+	+	+
Leech hyaluronidase	Hyaluronic acid	↓	+	+	+
Streptomyces hyaluronidase	Hyaluronic acid	↓	+	+	+
Chondroitinase ABC	Chondroitin 4- and 6-sulfate Dermatan sulfate Hyaluronic acid	↓↓	+	+	+
Chondroitinase AC	Chondroitin 4- and 6-sulfates Hyaluronic acid	↓↓	+	+	+
COLLOIDAL IRON STAINING					
Buffer control§		+	+‖	+	+
Testicular Hyaluronidase	Chondroitin 4- and 6-sulfates Hyaluronic acid	↓↓	+	+	+
Neuraminidase	Sialoglycoproteins Sialoglycolipids	+	+	−	−

* Results apply to both Tris and citrate-phosphate buffers.

‡ (+) Indicates staining is present, (−) indicates absence of staining, and (↓) indicates staining is decreased.

§ Acetate buffer.

‖ No distinct GAG particles are seen in the GBM after CI staining of 40-μm sections. However, because staining is concentrated in the laminae rarae and is removed (in the adult) by heparitinase, it is believed to be attributable to the presence of heparan sulfate.

MESANGIUM: The mesangial cells, like the endothelial cells, arise from the developing mesenchyme that "invades" the renal vesicle during the formation of capillary loops (Fig. 1). Initially, before endothelial fenestrae develop and lumina are open, these cells are difficult to distinguish from the endothelium. Later, upon maturation of the endothelium, they can be identified by their characteristic subendothelial location in axial regions. Because they do not normally occur along the peripheral or presumptive filtration surface of glomerular capillaries, they are not considered further here.

BASEMENT MEMBRANE: The earliest precursors of the GBM are recognizable during the S-shaped body stage and consist of (*a*) a 70–80-nm, loose, amorphous layer closely applied to the epithelial cell base (Figs. 2, 7, and 8); and (*b*) a corresponding layer closely applied to the endothelium (Fig. 7). Initially, these two layers are separated by extracellular (mesenchymal) matrix, but during the capillary loop stage, this matrix material is gradually eliminated and the two basement membrane layers blend, becoming progressively thicker and more electron dense (Figs. 9 and 10). Late in this stage, the three layers of the GBM (i.e., the lamina rara interna [LRI], the lamina densa, and the lamina rara externa [LRE]) become distinguishable, and the GBM assumes its mature dimensions (Figs. 11 and 12).

EPITHELIUM: We have described the differentiation of the epithelium in detail in a previous study (31). To summarize briefly, at the beginning of the S-shaped body stage, the presumptive visceral epithelium consists of columnar cells that are joined at their apices (facing the parietal epithelium) by occluding zonules; subsequently, these junctions progressively migrate from the cell apex to the base (facing the basement membrane) where they fragment into occluding fasciae and maculae located between developing foot processes. The latter are formed by interdigitation of the epithelial cells. With more elaborate interdigitation, fewer and fewer intercellular spaces between foot processes are closed by occluding junctions that gradually disappear, and normal foot process and slit architecture prevails (Figs. 13–15).

Experiments with Cationic Probes

CF (pI 7.3–7.5) GIVEN IN VIVO: We have recently reported (20) that in the mature glomerulus, when CF fractions with restricted isoelectric points

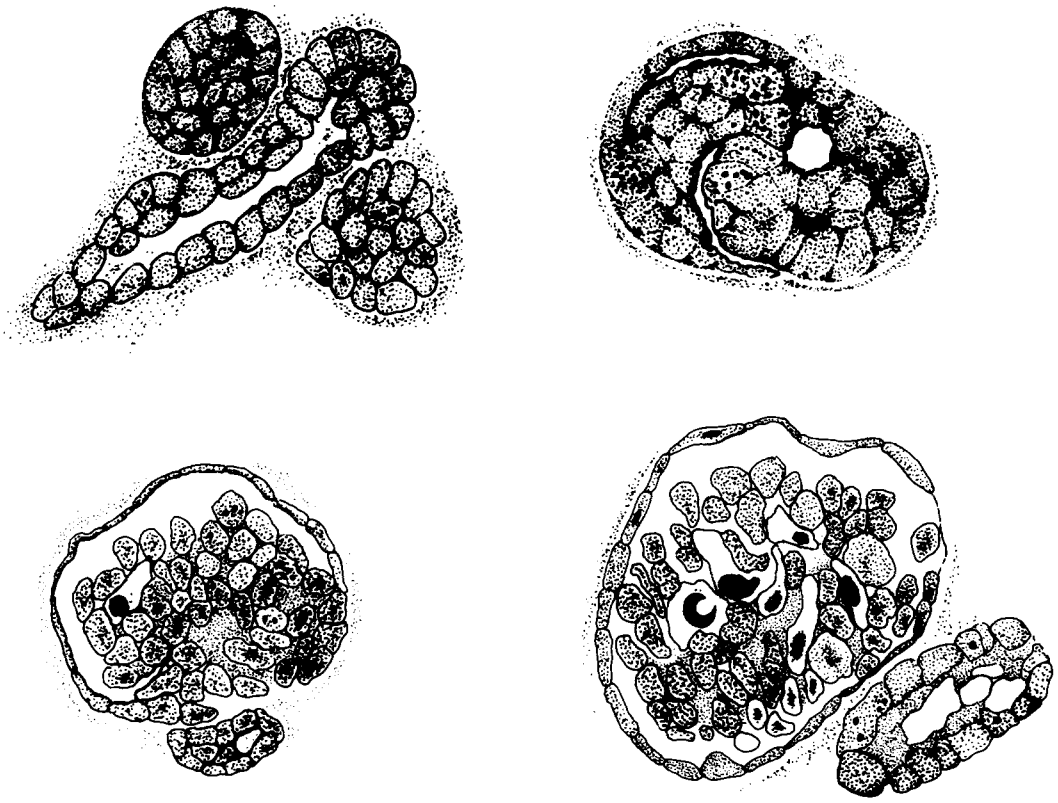

FIGURE 1 Diagrammatic representation of the four key stages in glomerular development as seen by light microscopy: the vesicle, the S-shaped body, the capillary loop, and the maturing glomerulus stages. The mammalian nephron is derived from two sources: the glomerulus and uriniferous tubule from the metanephric blastem and the collecting system from the ureteric bud (11). The terminal ampulla of the presumptive collecting duct (ureteric bud) induces formation of a renal vesicle, the earliest recognizable stage in glomerular differentiation, which consists of a cluster of cells that eventually develops a lumen. Here two renal vesicles are depicted on either side of a collecting duct (upper left). A cleft forms in the vesicle which is invaded by mesenchyme to form an S-shaped body (upper right). The cells on one side of the cleft (left side in the diagram) become glomerular epithelium and those on the other (to the right) become proximal tubule. Capillary endothelium and mesangium arise from the mesenchymal cells in the cleft. Their appearance leads to the formation of several capillary loops (lower left) with open lumens and circulating blood cells. With further development, in the maturing glomerulus (lower right) more capillary loops are formed, the layers become attenuated, and gradually organized into their adult form. (Redrawn from reference 31).

are prepared and used, CF is a very useful cationic probe for delineating anionic sites in the laminae rarae of the GBM. CF with a pI of 7.3–7.5 is optimal because, when it is given intravenously to adult rats, the CF molecules bind to anionic sites in the GBM, but they do not bind to anionic groups on the adjoining epithelial and endothelial cell surfaces (see Fig. 6).[2] When such a CF preparation is given to immature animals, its distribution within the glomerulus varies according to the stage of development (Figs. 3–6). In contrast to the situation in the adult glomerulus, before differentiation of the endothelial fenestrae,

[2] CF with a pI > 7.5 (which includes that available commercially from Miles Laboratories, Inc.) is not satisfactory for this purpose because it binds to cell surfaces of endothelia, erythrocytes, and platelets as well as to the sites in the GBM. The simplest interpretation of this observation is that the charge density of the heparan sulfate–rich sites in the GBM is greater than that of the sites (sialoglycoproteins and sialoglycolipids) on the cell surfaces.

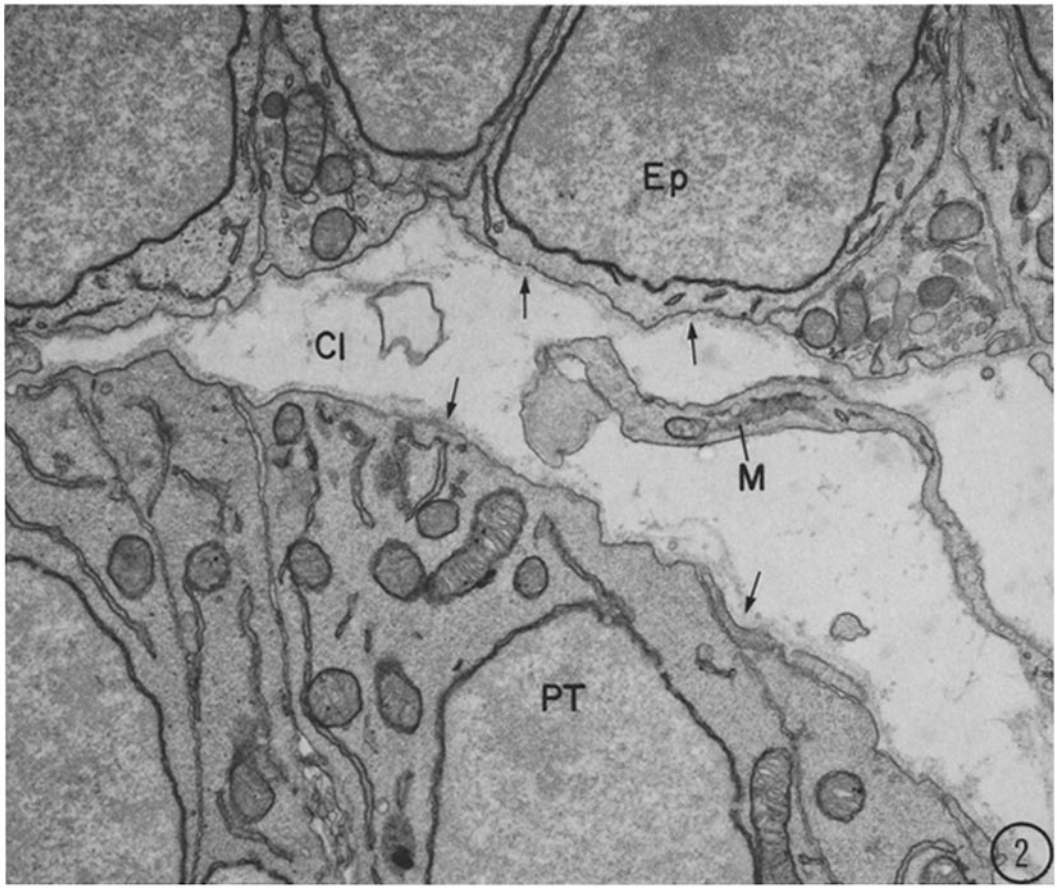

FIGURE 2 Low-power electron micrograph of the cleft region (*Cl*) of an S-shaped body (see Fig. 1, upper right) with the presumptive glomerular epithelium (*Ep*) on one side of the cleft and the proximal tubule epithelium (*PT*) on the other. Note the thin, moderately dense basement membrane layer (arrows) found along the surfaces of both epithelial layers separating them from the extracellular matrix. These layers represent the earliest recognizable precursors of the glomerular and tubular basement membranes. A portion of a mesenchymal cell (*M*) from which endothelium and mesangium form is also seen in the cleft. × 24,000.

CF binds to the endothelial cell surface where it occurs in a patchy distribution (Fig. 3). Upon appearance of fenestrae, CF binds in clusters to the thin diaphragms that close the earliest fenestrae (Fig. 4), indicating that these diaphragms contain a high concentration of negatively charged groups. At these stages, CF is infrequently found within the GBM; when present, it apparently gains access to the GBM either through occasional open fenestrae (Fig. 5) or through incomplete occluding junctions between endothelial cells. After disappearance of the fenestral diaphragms, CF readily penetrates the open fenestrae and is found throughout the GBM where it binds to negatively charged sites and is randomly distributed in clusters. It also passes through the GBM and reaches the intracellular spaces between the earliest developing foot processes (Fig. 5), but it is rarely found within the urinary spaces beyond. When the three layers of the GBM become recognizable, CF binds to anionic sites within the laminae rarae, as in the mature GBM (Fig. 6).

It can be concluded (*a*) that the early glomerular endothelium contains a high concentration of negatively charged groups along its luminal surface, (*b*) these negatively charged groups become concentrated along the fenestral diaphragms, (*c*) the diaphragms bind and restrict the passage of CF,

and (*d*) when the diaphragms disappear, CF enters the GBM through open fenestrae and either binds to anionic sites within the GBM, or passes through the GBM and is seen in the epithelial slits.

RR STAINING BY PERFUSION: This cationic dye has been extensively used to study anionic sites (cell coats) on cell surfaces (27), and proteoglycans in connective tissue matrices (17). It has also proved to be useful for delineating anionic sites in the GBM of mature rats (20) (see Figs. 11 and 12). In the developing glomerulus, RR is particularly useful during the S-shaped body stage because, when it is perfused (in contrast to CF), it readily gains access to the cleft and stains particles in the extracellular matrix (Figs. 7 and 8). Two types occur within the cleft: (*a*) small particles (10–15-nm) similar in appearance to those in the mature GBM, which are randomly distributed throughout the thin endothelial and epithelial basement membranes (Fig. 8); and (*b*) large (30-nm) particles or granules that are found in the cleft in the mesenchymal matrix between the two cell layers (Fig. 8). These larger granules appear to be associated exclusively with the S-shaped body because they appear within the cleft as soon as it forms, they do not occur in mesenchyme outside the cleft, and they are not seen in developing glomeruli much beyond this stage. Two types of fibrillar projections radiate from the large granules. Initially, short, thin (3–5-nm) spikes project from and interconnect the granules, forming a loose matrix, within the cleft (Figs. 7, 8, 17, and 18). Somewhat later, thicker (10-nm) fibrillar projections are present, and these thick fibrils remain between the endothelial and epithelial basement membranes after the 30-nm granules begin to disappear (Fig. 9).

After fusion of the epithelial and endothelial basement membranes, the large granules are no longer seen, but the smaller (10–15-nm) granules persist, randomly distributed within the GBM (Fig. 10). As the GBM organizes into its characteristic three layers, the small granules become arranged in their mature configuration in the LRI and LRE (Figs. 11 and 12). As in the adult, the small particles are best demonstrated when the dye is perfused in the fixative, but they can also be visualized (although less well) in ~40-μm sections immersed in the dye. As indicated, they are identical in morphology and distribution to the heparan sulfate–rich, proteoglycan particles found in mature glomeruli (20, 21), except that in the immature glomerulus, they are smaller (10–15 as compared to 20 nm) and are spaced closer together (40–45 as compared to 60 nm).

CI: CI staining carried out at pH 1.6 (33) stains primarily or exclusively sialic acid groups and GAG in the glomerulus (21, 23). This technique has been extensively used to study the so-called epithelial polyanion, i.e., the rich, negatively charged cell surface coat found on the visceral epithelium (19, 29, 30). When positive CI-staining is detected in glomeruli by light microscopy, it has often been incorrectly interpreted as resulting exclusively from epithelial staining (6), in spite of the fact that results obtained by electron microscopy clearly reveal that negatively charged groups in the GBM (19, 23) and on endothelial cell surfaces (23) stain with CI as well.

When 40-μm sections from the newborn rat kidney are stained with CI and examined with the electron microscope (Figs. 13–15), it is evident (confirming light-microscope findings [31]) that when the occluding junctions are still located at the cell apex (vesicle and S-shaped body stages), staining of the visceral epithelium is minimal. Coinciding with the beginning of junctional migration to the epithelial cell base (capillary loop stage), heavy CI-staining appears along the lateral cell surfaces above the level of the occluding junctions (Figs. 13 and 14). The deposits of CI are distributed in a globular pattern that is best seen in grazing sections (Fig. 14). The remainder of the epithelial cell surface (i.e., the lateral membrane below the level of the occluding junctions and the basal membrane of the foot processes) is not stained; however, the adjacent GBM is diffusely stained with CI (Fig. 15), as in the adult (21, 23). With beginning interdigitation of the epithelium, this pattern of staining of the cell membrane is maintained: the membranes of the earliest foot processes that are joined by focal occluding junctions are stained by CI above but not below the level of the junctions (Fig. 14). After disappearance of the focal occluding junctions, staining is seen along the lateral aspects of the foot processes; however, little or no staining is ever seen at their base (Figs. 13 and 15).

CI staining appears along the endothelial cell surface facing the capillary lumen at about the same time as that along the epithelium; however, the extent of CI staining of the endothelium is much less. As in the case of the epithelium, the domain of the endothelial cell facing the GBM does not stain with CI under these conditions (Figs. 13 and 14).

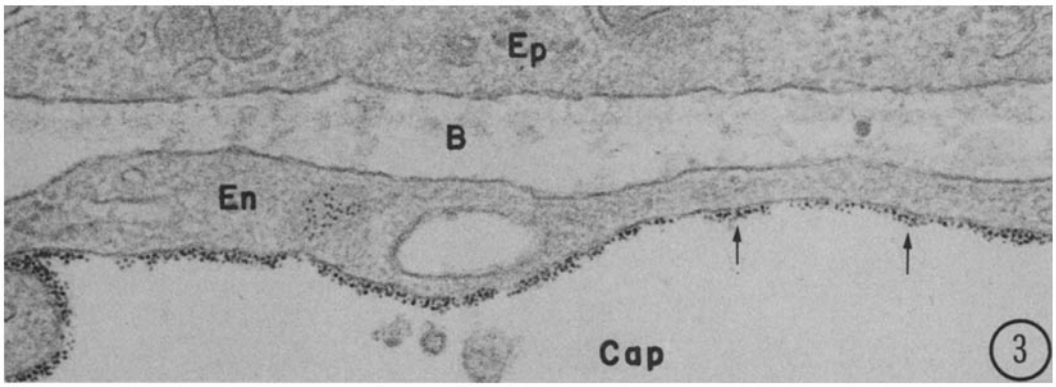
Ep
B
En
Cap
3

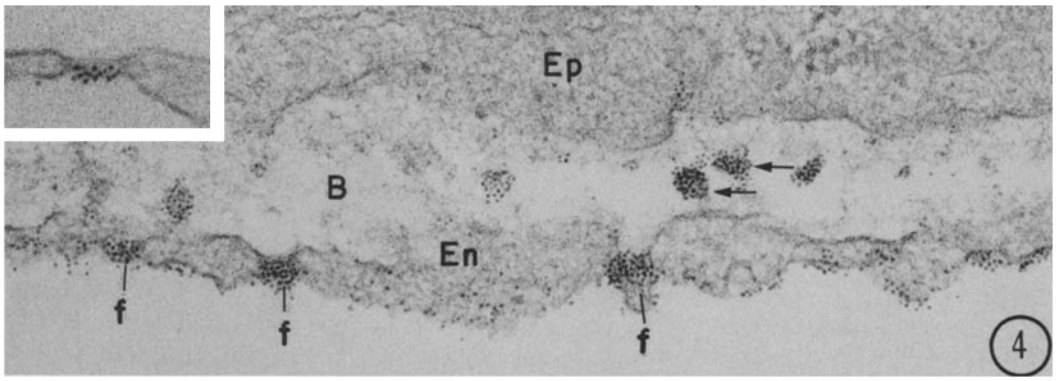
Ep
B
En
f
f
f
4

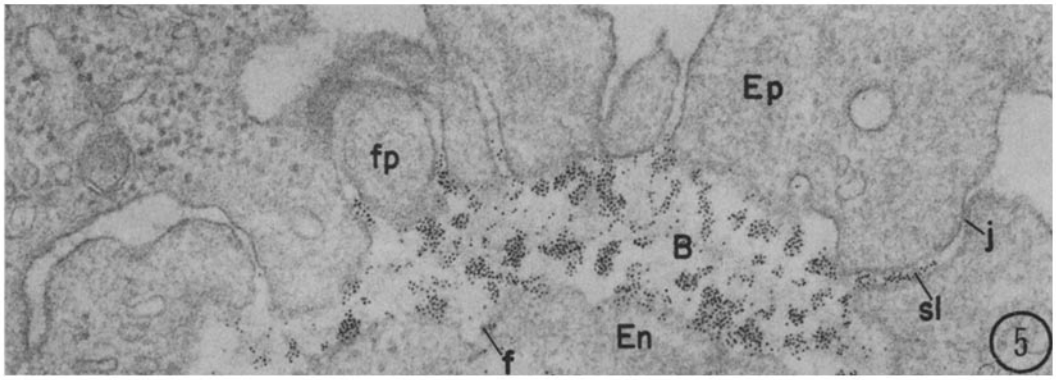
Ep
fp
B
j
sl
En
f
5

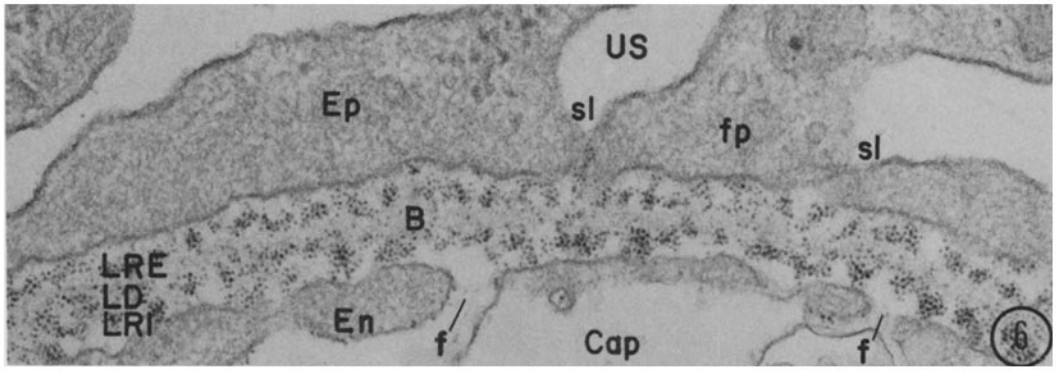
US
Ep
sl
fp
sl
B
LRE
LD
LRI
En
f
Cap
f
6

The pattern of CI-staining in the GBM and its forerunners varies with the stage. In the S-shaped body stage, the large (30-nm) granules found within the cleft stain with CI, and the epithelial and endothelial basement membranes contain a diffuse CI precipitate. As the GBM matures, increasing amounts of CI are seen concentrated within the laminae rarae in a fairly even distribution, with the deposits being much heavier in the LRE than in the LRI (Fig. 15). The small (10–15-nm) particles are not evident.

Enzyme Digestion Studies

Immature glomeruli were subjected to digestion with enzymes that digest sialic acid (neuraminidase) and specific GAG, to gain information on the nature of anionic sites in the developing glomerulus. The results are summarized in Table I and are described below.

EFFECTS OF ENZYME TREATMENTS ON CI-STAINED SITES: CI staining of the epithelial and endothelial cell surfaces was not seen in specimens digested with neuraminidase (Fig. 16), but was present and apparently unaffected after digestion with testicular hyaluronidase. Staining of the GBM was not affected by either enzyme. Because it is specifically removed by neuraminidase, we can conclude that the CI staining of the cell surfaces in developing glomeruli is a result of the presence of sialic acid, presumably in membrane sialoglycoproteins or sialoglycolipids, as in the adult glomerulus (19, 29). That the GBM staining is not affected by digestion with either of these enzymes, which together remove sialic acid and all sulfated GAG except heparan sulfate, indicates that it most likely results from the heparan sulfate that is concentrated in the laminae rarae (see below).

EFFECTS OF ENZYME TREATMENTS ON RR-STAINED SITES: The large (30-nm) granules prominent in the cleft of the S-shaped body were partially removed by incubation in chondroitinase ABC (Fig. 20), chondroitinase AC (Fig. 22) and by streptomyces (Fig. 19) and leech (Fig. 21) hyaluronidases. Staining of the granules in controls (Figs. 17 and 18) incubated in buffer alone was unaffected. That staining of the 30-nm granules was affected by two enzymes (hyaluronidases) that specifically remove hyaluronic acid indicates that the granules contain this GAG. After examining many electron micrographs, we have come to the conclusion that removal of the particles is more extensive with chondroitinases AC and ABC (which remove both hyaluronic acid and chondroitin sulfate) than with leech or streptomyces hyaluronidases (which remove only hyaluronic acid). This suggests that both hyaluronic acid and chondroitin sulfate may be present in the granules.

The smaller (10–15-nm) granules were not removed by any of these enzymes that collectively remove all GAG except heparin and heparan sulfate, a finding that supports our assumption that the granules are precursors of the heparan sulfate–rich proteoglycan granules found in the mature GBM. The latter can be specifically removed by heparitinase (or by nitrous acid oxida-

FIGURES 3–6 Distribution of CF (pI 7.3) in developing glomeruli early (Figs. 3–4), middle (Fig. 5), and late (Fig. 6) in the capillary loop stage. In Fig. 3, before the development of endothelial fenestrae, CF binds in a patchy distribution (arrows) to the luminal side of the endothelium (*En*) and does not reach the GBM (*B*) or epithelium (*Ep*). A capillary lumen is marked (*Cap*). In Fig. 4, endothelial fenestrae (*f*) have appeared and CF binds in large amounts to the diaphragms that close these early fenestrae. Small amounts of CF are also found in the GBM (*B*) binding in clumps to large proteoglycan particles (arrows). CF gains entry to the GBM either through open fenestrae (lacking diaphragms) or through open junctions between endothelial cells located outside the plane of section. The *inset* (upper left) shows another fenestra with bound CF in which the diaphragm is clearly visible. In Fig. 5, open fenestrae are present (*f*), and CF has gained access to the GBM (*B*) and the intercellular spaces between developing foot processes (*fp*). Considerable CF is bound to anionic sites in the GBM. At this stage many of the epithelial slits are sealed by focal occluding junctions (*j*) that are located at some distance from the GBM. A filtration slit is marked (*sl*). In Fig. 6, open fenestrae (*f*) are more frequent, and the GBM has become organized into its characteristic three layers. CF binds to anionic sites concentrated in the laminae rara interna (*LRI*) and externa (*LRE*). Epithelial foot processes (*fp*) and filtration slits (*sl*) are present at this stage. Note that no CF is seen within the urinary spaces (*US*) or binding to the epithelial (*Ep*) surfaces. Binding to the endothelium (*En*) is minimal compared to previous stages. *Cap*, capillary lumen; *LD*, lamina densa. Figs. 3, 4, and 6, × 75,000; Fig. 5, × 54,000; *inset*, × 110,000.

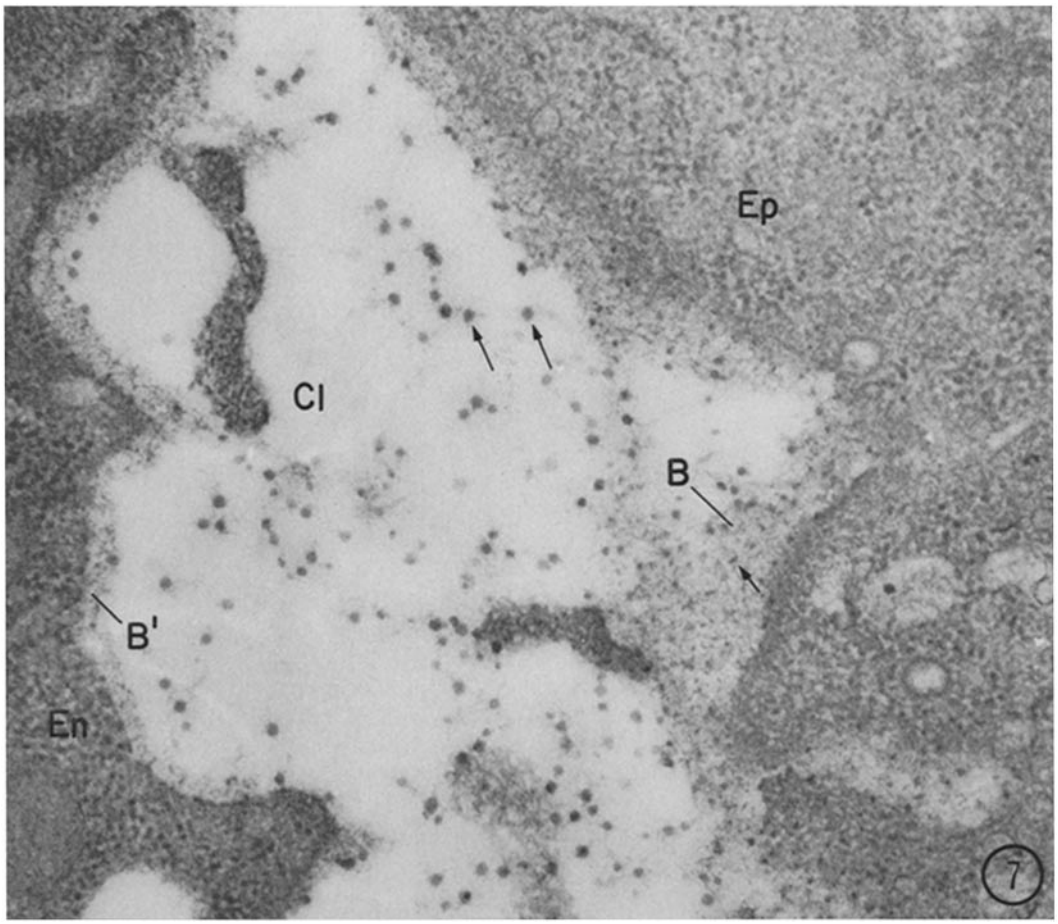

FIGURE 7 Cleft of an S-shaped body from a kidney perfused with RR. RR gains access to the cleft (*Cl*) and stains numerous large (30-nm) proteoglycan particles (long arrows) located in the mesenchyme between the presumptive epithelium (*Ep*) and endothelium (*En*). Spikelike projections radiate from and interconnect the granules, forming a loose matrix within the cleft (see Figs. 17–18). Smaller (10–15-nm) granules (short arrow) are found within the loose epithelial (*B*) and endothelial (*B'*) basement membranes. × 69,000.

tion), but are not affected by other GAG-specific enzymes (21).

On the basis of these cytochemical studies, it seems likely that the larger (30-nm) granules contain a mixture of hyaluronic acid and chondroitin sulfate, whereas the smaller (10–15-nm) granules consist of heparan sulfate. Both types of granules can be assumed to consist of proteoglycans (i.e., protein-polysaccharide complexes), because (except for hyaluronic acid) GAG do not ordinarily occur alone in tissues (17, 26).

RR staining of epithelial and endothelial cell surfaces is unaffected by digestion with leech or streptomyces hyaluronidases, or chondroitinase ABC or AC under the conditions employed, suggesting that this staining results from the presence of acidic groups other than hyaluronic acid, dermatan, or chondroitin sulfates.

Experiments with NF

NF (pI = ~4.8) has frequently been used as an electron-dense tracer to study glomerular permeability (12, 14). In the mature glomerulus, when NF is administered intravenously, molecules of the tracer penetrate the endothelial fenestrae and reach the LRI, but fail to enter the lamina densa and to penetrate beyond this level to any extent (see Fig. 24).

When NF is administered intravenously to neonatal rats, its distribution varies with the stage of development. Before development of endothelial fenestrae and disappearance of their diaphragms, it fails to gain access to the cleft of the S-shaped body. After a few open fenestrae appear and before the GBM is mature, molecules are found in small amounts throughout the LRI and lamina densa. Unlike CF, NF is found all around the capillary loop, indicating that it diffuses more readily within the plane of the GBM than CF, which is not surprising because, being anionic, it is not trapped by binding to negatively charged sites. At this time, NF is found more or less evenly distributed throughout the inner two-thirds of the GBM with little difference in the concentration of tracer in the LRI as compared to the lamina densa (Fig. 23). Thus, the concentration gradient across the GBM is less marked and the lamina densa is apparently more porous than at later stages. After the three layers of the GBM become evident (Fig. 24), an increasing gradient is seen in the lamina densa, i.e., the tracer is present in much larger amounts within the LRI than within the lamina densa. However, the GBM still appears to be more permeable to NF than the mature GBM because more molecules of the tracer are found within the lamina densa than in the mature glomerulus, and occasionally molecules are even seen within the urinary spaces.

It appears, therefore, that there is a progressive decrease in the penetration of NF into the GBM (as manifested by an increasing gradient of ferritin concentration) as the GBM matures and the lamina densa becomes recognizably thicker and more compact. This coincides with the appearance of increasing numbers of open endothelial fenestrae, the arrangement of the small proteoglycan granules into two layers within the laminae rarae, and the formation of foot processes and filtration slits.

DISCUSSION

We have used a variety of cationic probes, specific enzymes, and the anionic tracer, ferritin, to study the assembly of the glomerular filtration surface and its function in the newborn rat glomerulus. During development, the three layers of the glomerulus differentiate synchronously to form the mature filtration surface. The immature GBM is more permeable than the mature GBM to both native (pI = 4.8) and cationic (pI = 7.3) ferritin; yet despite the fact that the charge and size selectivity of the GBM is poorly developed, proteinuria is minimal at all stages of development (11). Our findings indicate that when the GBM is immature, access to it is regulated by the relative scarcity of open endothelial fenestrae and exit from it by the paucity of patent epithelial slits. This is consistent with the functional model of glomerular filtration proposed some time ago (14; reviewed in reference 12) according to which it is assumed that the cellular layers can modulate the behavior of the GBM, a point developed further in the appropriate sections below.

Development of Endothelial Fenestrae

A new finding in this study is that the earliest fenestrae that appear in the previously continuous endothelial layer possess diaphragms resembling those of the endothelial fenestrae of intestinal capillaries in the adult in their ability to restrict passage of native (anionic) ferritin (9) and in their binding of CF (37), indicating a high concentration of anionic groups. In the case of the intestinal capillaries, the anionic groups concentrated on the endothelial diaphragms have been identified as heparan sulfate (37). In the immature glomerulus, fenestral diaphragms are present only transiently, because open fenestrae (lacking diaphragms) soon appear.

The opening of the fenestrae parallels the development of a more compact GBM that is increasingly able to serve as a barrier to anionic proteins (i.e., NF). Thus, the endothelium regulates access to the GBM at stages during which the filter is imperfect, (*a*) by regulating the number of fenestrae, and (*b*) by the presence of fenestral diaphragms that, like those of other endothelia (37), are highly negatively charged and prevent access of anionic macromolecules to the GBM. As the glomerulus matures, both the total number of fenestrae and the proportion of open fenestrae gradually increases. In this way, the total area of the GBM directly exposed to the plasma is controlled (12, 14).

Development of the GBM

Previous work on embryonic kidneys (11, 40, 45) has established that the mature GBM is assembled by mergence and maturation of the basement membranes of the presumptive glomerular endothelium and epithelium with gradual elimination of the intervening mesenchymal matrix. We have studied the appearance of anionic sites in the GBM, using RR and CF. A new finding that has emerged is the identification of two types of GAG

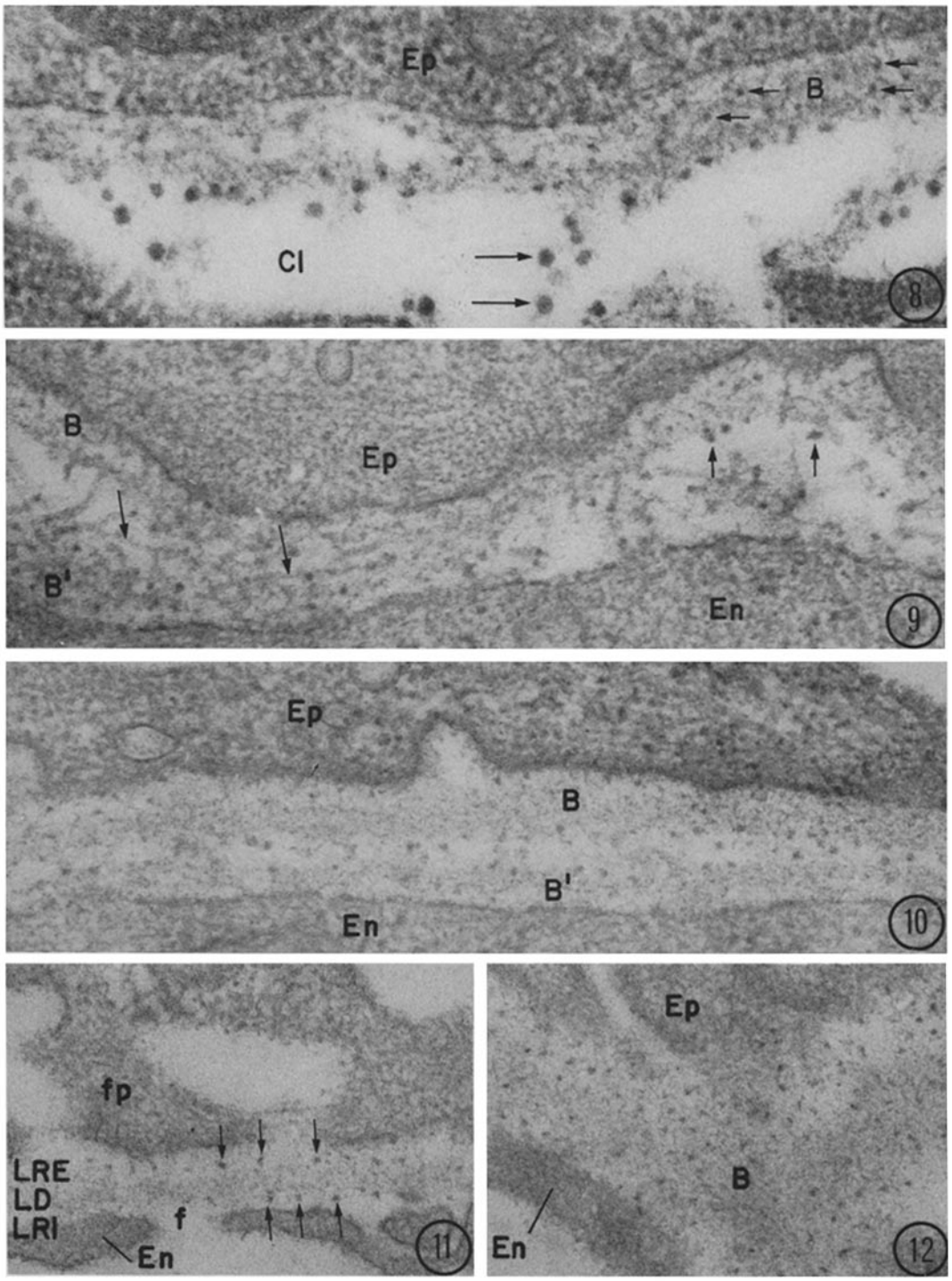
Ep
B
Cl
8
B
Ep
B'
En
9
Ep
B
B'
En
10
fp
LRE
LD
LRI
f
En
11
Ep
B
En
12

granules: (*a*) smaller (10–15-nm) granules or particles found in the developing GBM at all developmental stages, and (*b*) large (30-nm) granules found in the mesenchymal matrix of the cleft only during the S-shaped body stage. Both are presumed to be proteoglycans (26).

SMALL PROTEOGLYCAN GRANULES: These granules are first seen randomly distributed within the epithelial and endothelial basement membranes in the S-shaped body stage; they remain randomly distributed throughout the common, presumptive GBM after the two basement membranes fuse, and eventually become concentrated within the laminae rarae. Given the morphology of the particles, their location (in the laminae rarae), and their lack of sensitivity to digestion by any of the enzymes used (which would be expected to remove all GAG except heparin or heparan sulfate), it can be reliably assumed that they represent the precursors of the heparan sulfate–rich proteoglycan granules recently demonstrated in the GBM (both *in situ* and isolated GBM [20, 21]).[3] The precise function of these granules remains to be established, but several possibilities have been considered elsewhere (13, 20, 21). The reason for the smaller size of these granules in developing glomeruli as compared to mature glomeruli (10–15 nm vs. 20 nm) is not known. It could indicate that the overall size of the proteoglycan aggregates is smaller or, alternatively, it could be a preparatory artifact characteristic of immature, less compact GBM.

30-nm GRANULES: These large GAG granules appear in the cleft of the S-shaped body just before the extensive vascularization that results from proliferation of mesenchymal cells and gives rise to the endothelium and mesangium. From the results of RR staining and digestion with specific enzymes, it appears that these granules contain hyaluronic acid (based on their partial removal with specific hyaluronidases) and perhaps chondroitin sulfate as well (based on their more extensive removal with chondroitinases ABC and AC as compared to streptomyces and leech hyaluronidases). The timing of the appearance of hyaluronic acid–rich granules within the cleft of the S-shaped body just before mesenchymal invasion and their rapid disappearance is of considerable interest in view of the findings of Toole and co-workers (41–43), and Bernfield et al. (4, 10), which suggest that hyaluronate may act as an extracellular signal during embryonic development. Hyaluronate synthesis is closely correlated with cell differentiation. The large granules resemble, in their appearance after RR staining and their susceptibility to digestion with various enzymes, proteoglycan granules

[3] We have recently obtained evidence that they are necessary for maintenance of the normal permeability properties of the GBM, because removal of GAG (heparan sulfate and hyaluronic acid) by digestion with heparinase results in increased permeability of the GBM to native ferritin (Kanwar, Y. S., and M. G. Farquhar. 1979. Kidney Int. **16**:823.

FIGURES 8–12 These figures show successive stages in the maturation of the GBM in preparations stained with ruthenium red (RR). Fig. 8, from the S-shaped body stage, illustrates side by side the two types of RR-stained proteoglycan particles: large (30-nm) granules located within the cleft (*Cl*) (long arrows) and smaller (10–15-nm) ones (short arrows) located within the epithelial basement membrane (*B*). Fig. 9, from the beginning of the capillary loop stage, shows what appear to be vestiges of large particles (short arrows) that are faintly stained and interconnected by thicker (10-nm) strands (long arrows) than those seen during the S-shaped body stage (see Fig. 7). These thick fibrils form a meshwork within the spaces destined to become the lamina densa. Smaller (10–15-nm) particles are also seen within the epithelial (*B*) and endothelial (*B'*) basement membrane. Note the dense feltwork of fibrils (actin?) in the cytoplasm of the epithelial cell (*Ep*). Fig. 10, from the middle of the capillary loop stage, shows the epithelial (*B*) and endothelial (*B'*) basement membranes coming close together, separated by only a thin layer of residual mesenchyme. Small (10–15-nm) RR-stained particles are seen throughout both basement membranes at this stage. Figs. 11 and 12, from late in the capillary loop stage, show the GBM when it is nearly mature and is organized into its characteristic three layers: the lamina rara interna (*LRI*), the lamina densa (*LD*), and the lamina rara externa (*LRE*). The small (10–15-nm) proteoglycan particles (arrows) are distributed in two layers restricted to the laminae rarae. As in the adult (20), these granules form a quasi-regular network that is best seen in grazing sections (Fig. 12). Note that at this stage, the endothelium (*En*) and epithelium (*Ep*) are virtually the same as in the adult, with open fenestrae (*f*), foot processes (*fp*) and filtration slits being present. × 90,000.

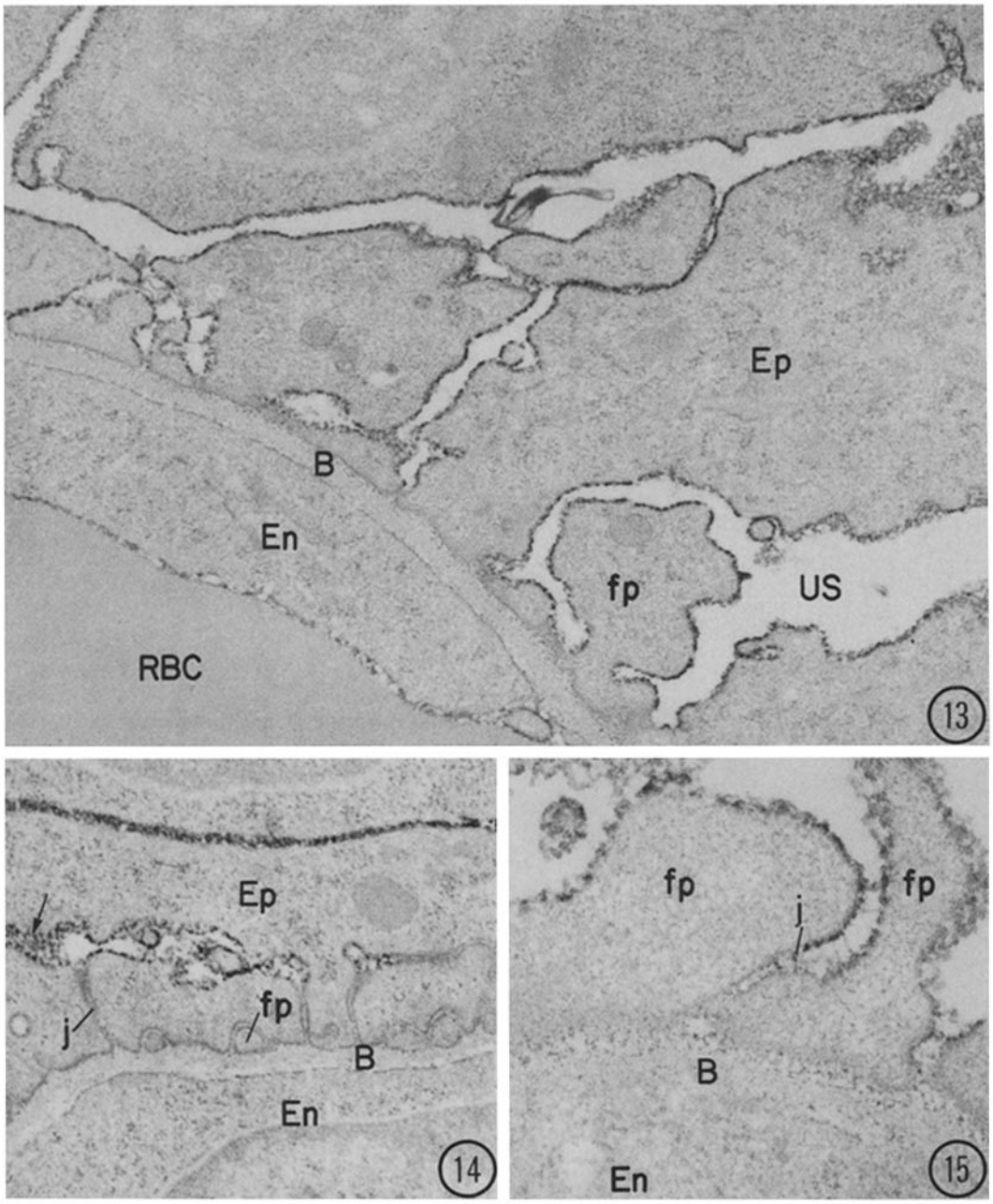

FIGURES 13–15 Distribution of colloidal iron; capillary loop stage. Dense deposits are present on the plasma membrane of the epithelium (*Ep*), the endothelium (*En*) and in the laminae rarae (interna and externa) of the GBM (*B*). Staining is particularly heavy on the epithelium. Note that in all three figures the basal surface of the presumptive foot processes (*fp*) where they face the GBM as well as the surface of the endothelium facing the GBM is not stained although deposits are seen in the adjacent GBM (Fig. 15). In Fig. 13, the erythrocyte (*RBC*) within the capillary lumen also has a CI-stained, cell surface coat. *US*, urinary space. Figs. 14 and 15 demonstrate that where occluding junctions (*j*) remain, the lateral cell surfaces of the earliest foot processes (*fp*) stain with CI only above the level of the junctions. The irregular, lumpy distribution of CI on the epithelial cell surface is best seen in grazing section in Fig. 14 (arrow). Figs. 13 and 14, × 30,000; Fig. 15, × 69,000.

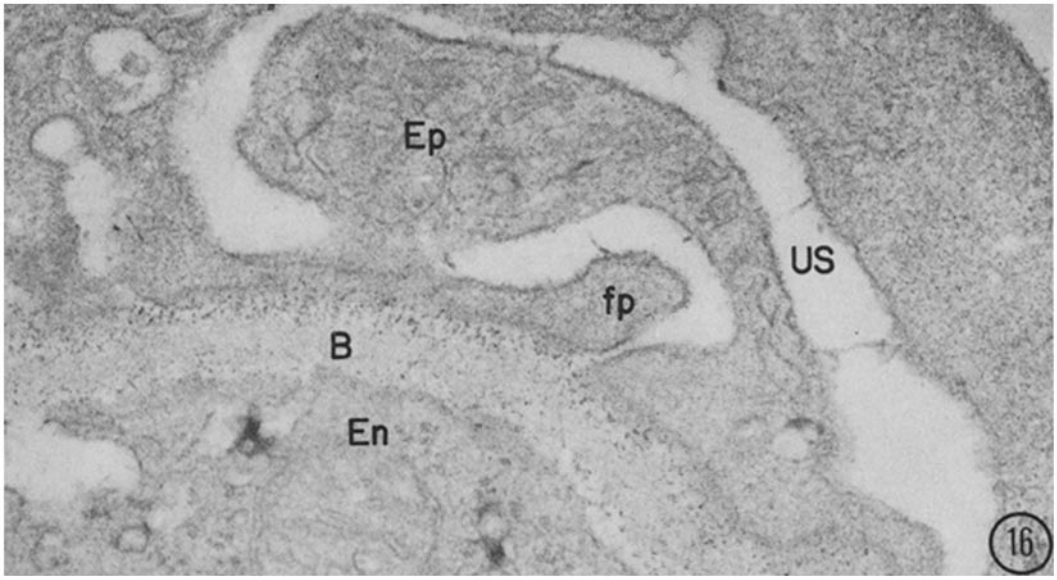

FIGURE 16 Portion of a glomerulus in the capillary loop stage from a specimen incubated with neuraminidase (8 h) before being stained with colloidal iron. No CI staining is seen on the membranes of either the epithelium (*Ep*) (including that of the foot processes [*fp*]), or endothelium (*En*). Staining of the laminae rarae of the GBM (*B*) is present and apparently unaffected by the enzyme treatment. *US*, urinary space. × 69,000.

found in mature cartilage (2, 17) and in other embryonic connective tissues (16, 17, 44). Such large proteoglycan granules are particularly abundant in embryonic extracellular matrices where, like the granules in the developing glomerulus, they are typically interconnected by fibrillar networks (~4-nm microfibrils and ~10-nm nonstriated fibrils) (17). The nature of the fibrils is uncertain, but it has been suggested by Hay et al. (17) that they represent variations or precursors of collagen fibrils.

Except for the cytochemical data mentioned, little information is available concerning the biochemical composition or physical properties of either the large proteoglycan particles common in embryonic connective tissue matrices or the smaller, heparan sulfate–rich, presumptive proteoglycan particles found in the GBM and in other renal basement membranes (13). The best-studied proteoglycan from this standpoint is the chondroitin sulfate proteoglycan of the cartilage matrix, which according to the data available, forms complex aggregates by interaction of monomers composed of a central protein core from which radiate sulfated GAG (chondroitin sulfate and keratan sulfate) with hyaluronic acid and/or link protein (18, 25, 34). Hyaluronic acid is believed to hold several proteoglycan molecules together to form an aggregate (18, 25). If a comparable situation exists in the large (30-nm) granules found in extracellular matrices, removal of either hyaluronic acid or link protein (e.g., by enzymatic digestion) might cause the aggregate to fall apart with loss of the remaining components.

ASSEMBLY OF THE GBM: Based on our findings and on what is known at present of the composition and assembly of extracellular matrix components, a working hypothesis for the assembly of the GBM can be proposed: the large granules within the cleft may represent an aggregate of proteoglycan monomers (such as those of cartilage matrix) rich in hyaluronic acid and chondroitin sulfate, which may serve both as a signal for migration of mesenchymal cells into the cleft of the S-shaped body and as a template for the formation of the large, nonbanded fibrils (such as those seen in Fig. 17), which are assumed to be collagenous in nature. The latter is in keeping with the fact that the nature and amount of GAG present in extracellular matrices is known to influence the macromolecular organization of collagen (15, 25, 26). The loss of the large granules early in the capillary loop stage is most likely a result of the action of a local hyaluronidase, known to be

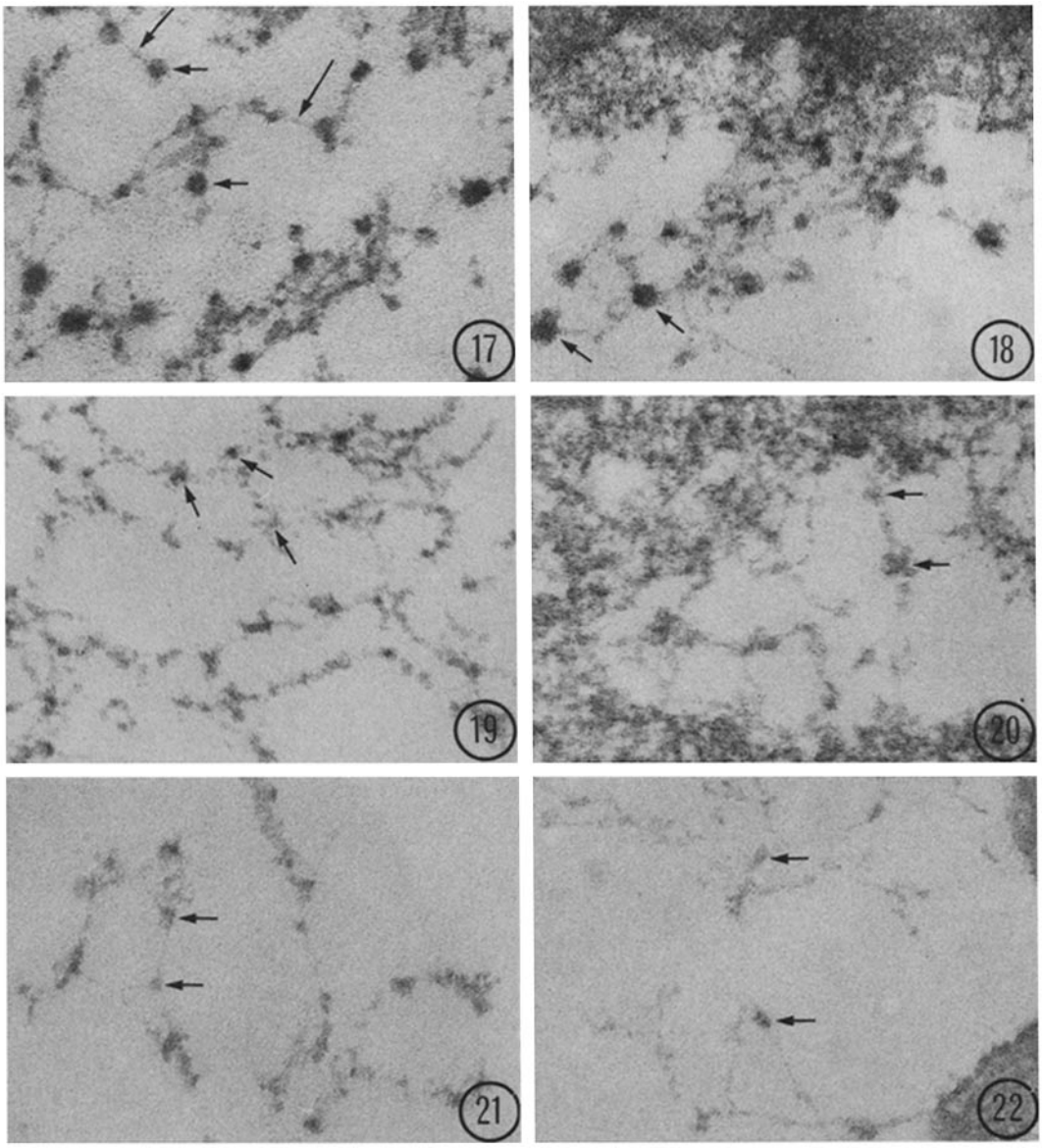

FIGURES 17–22 These figures illustrate the effect of digestion with specific enzymes on the 30-nm, RR-stained granules in the cleft of the S-shaped body. Figs. 17 and 18 are controls incubated in citrate-phosphate (pH 5.6) and Tris buffer (pH 8.0), respectively. The granules are deeply stained by RR (short arrows) and are interconnected by fibrils. Many of the latter show a central density (long arrows). Figs. 19 and 21 are from specimens incubated in *Streptomyces* and leech hyaluronidase, respectively, and Figs. 20 and 22 are from preparations incubated in chondroitinase ABC and AC, respectively. In all these specimens the large granules (arrows) appear much smaller and their staining is greatly reduced over controls, suggesting that the particles are partially digested by the enzyme treatments. Staining of the interconnecting fibrils is apparently unaffected. × 110,000.

high in developing systems (41). The digestion of the large granules leaves only the large fibrils within the space destined to become the lamina densa. As maturation progresses and the endothelial and epithelial basement membranes fuse, these fibrils are no longer recognizable, which could be

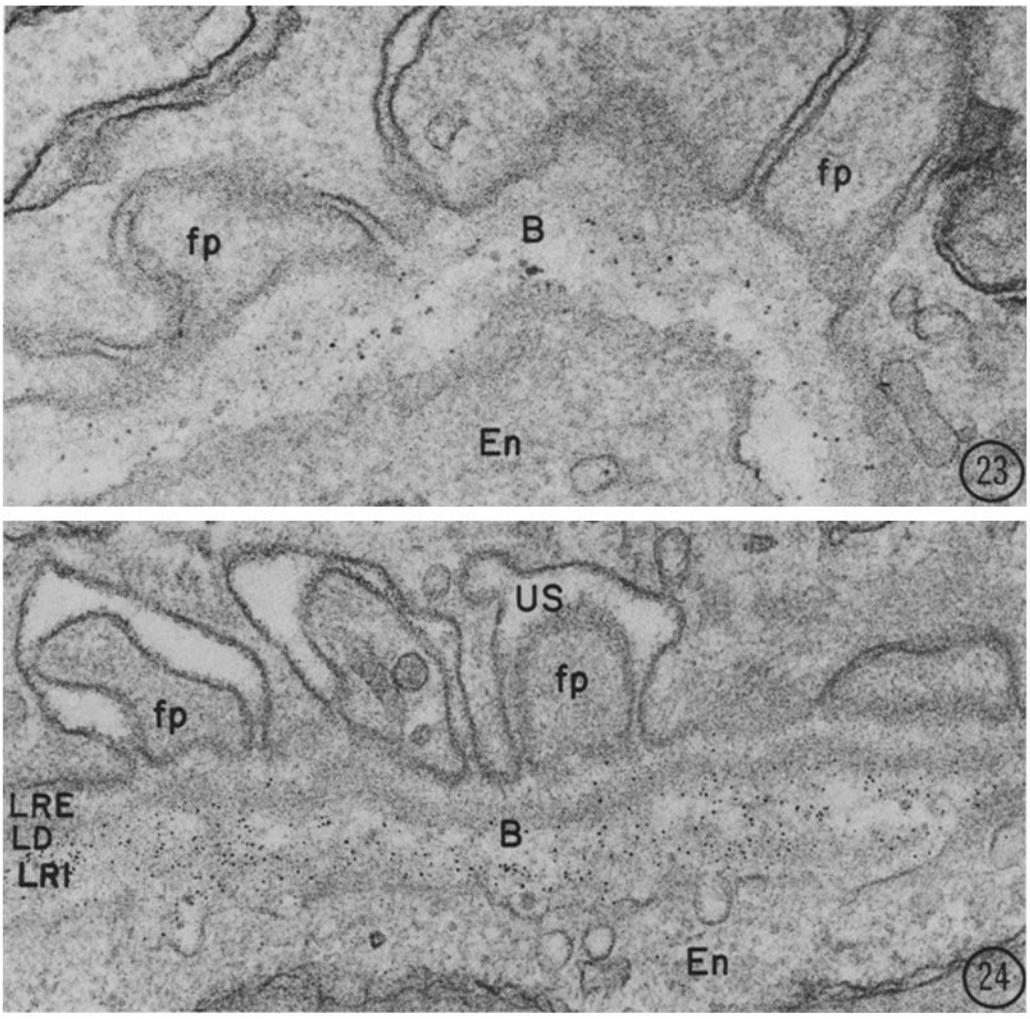

FIGURES 23–24 These two fields are from kidneys of newborn rats fixed 15 min after intravenous injection of native ferritin. Fig. 23 shows that early in the capillary loop stage, before three distinct layers are seen in the GBM, ferritin molecules are scattered randomly throughout the inner two-thirds of the rather loose-appearing GBM (*B*). The endothelium (*En*) is thick and contains relatively few fenestrae. Little or no ferritin is seen in the outer one-third of the GBM, indicating that although the lamina densa appears rather loose and irregular, it provides a barrier to the free penetration of ferritin. Fig. 24 shows another field later in the same stage. The three layers of the GBM have differentiated and the lamina densa (*LD*) has become arranged in a more compact layer. At this time, the barrier function of the GBM becomes more evident, because a distinct concentration gradient is seen with much larger amounts of ferritin being present in the LRI as compared to the LD. Counts of ferritin particles confirm that whereas a gradient is present in both figures, a much greater percentage of the total ferritin present in the GBM (20% as opposed to 5%) is seen in the outer half of the GBM in Fig. 23 as compared to Fig. 24. However, even in Fig. 24, the GBM is leakier than in the adult because in the adult, ferritin molecules are seldom seen beyond the LRE. × 75,000.

attributable to their (*a*) removal (digestion), (*b*) further modification (e.g., glycosylation or cross-linking), or (*c*) masking by secretion of additional GBM components. At the same time, the small proteoglycan particles persist and are displaced and segregated into the laminae rarae as the lamina densa becomes increasingly compact. In the future it will be of interest to take advantage of

the availability of specific antibodies to the various types of collagens (39) and to at least some proteoglycans (47) to study the assembly of the GBM by immunocytochemistry.

Development of Epithelial Slits and Epithelial Polyanion

MAINTENANCE OF DIFFERENT EPITHELIAL PLASMALEMMAL DOMAINS: We have shown that the CI-stained, neuraminidase-sensitive, epithelial polyanion first forms at the apical cell surface during the S-shaped body stage, extends down the lateral cell surfaces (to the level of the junctions) as the occluding junctions migrate toward the cell base, and appears on the foot processes only after disappearance of the focal occluding junctions from the presumptive filtration slits. Thereafter the entire epithelial cell surface is heavily stained except for that at the base of the foot processes. Thus, our findings provide evidence for the existence of distinctive sialic acid–rich, and sialic acid–poor plasmalemmal domains on the epithelial cell surface. The maintenance of the different domains early in development correlates with, and apparently relies upon, the existence of occluding junctions. After disappearance of the junctions, differentiated domains persist and are maintained in the plane of a continuous membrane, as staining at the base of the foot processes differs from that along the remaining cell surface. The existence of membrane specialization in the absence of junctional devices must involve some additional mechanism (cytoskeletal network?) similar to the spectrin-actin network of the erythrocyte membrane (38). A similar differentiation into sialic acid–rich and sialic acid–poor plasmalemmal domains also exists on the endothelium (see Fig. 13) because the basal cell membrane (facing the GBM) does not stain with CI, whereas the remainder of the endothelial surface does.

FORMATION OF FOOT PROCESSES AND FILTRATION SLITS: We have shown that in developing glomeruli the intercellular spaces between adjoining visceral epithelial cells are initially closed by occluding zonules (31) and, as the junctions migrate to the cell base and fragment into occluding maculae, epithelial polyanion and widened intercellular spaces appear above the level of the migrating junctions. The appearance of polyanion along the lateral cell surfaces near the GBM coincides with the appearance of interdigitation between adjoining cells, but CI staining of the lateral aspects of the foot processes and normal slit architecture are seen only after elimination of occluding maculae. These findings indicate that (*a*) opening of the epithelial slits by elimination of occluding junctions (like the opening of the endothelial fenestrae) parallels the development of a more compact, GBM, and (*b*) staining for epithelial polyanion and presence of normal slit architecture go hand in hand. The latter is in keeping with other evidence (3, 29, 36) indicating that epithelial polyanion is necessary for the maintenance of normal foot process and slit architecture.

Permeability of the Developing GBM to NF

In the mature glomerulus, the ferritin concentration drops off sharply in the LRI, and relatively few molecules reach the deeper layers (lamina densa and LRE) of the GBM (14, 32). The GBM of immature glomeruli is more permeable to NF than is the mature GBM because initially (early in the capillary loop stage), ferritin penetrates the lamina densa to a greater extent suggesting that the barrier function of the GBM—both its size- and charge-selective properties—is poorly developed. Later on (toward the middle of this stage), the GBM becomes increasingly capable of serving as a restrictive barrier to proteins because the gradient of ferritin concentration becomes more pronounced as maturation progresses. As the GBM becomes increasingly functionally competent, the number of endothelial fenestrae and frequency of open epithelial slits (lacking occluding junctions) steadily increases. Thus, it appears that the synchronous development of the cell layers permits the gradual establishment of glomerular filtration by regulating access to and exit from the GBM before the GBM is fully developed. Only when the GBM becomes organized into an effective barrier to the passage of protein molecules do the total area of the GBM directly exposed to the blood plasma through open endothelial fenestrae and the total exit pathway represented by the collective slit area reach their normal levels (~20% of the GBM surface [14]).

We wish to thank Bonnie Peng, Nancy Bull, and Barbara Dannacher for preparation of thin sections, Pam Ossorio for photographic assistance, and Lynne Wootton for editorial and secretarial help.

This work was supported by U. S. Public Health Service research grant AM 17724 (to M. G. Farquhar).

The content of this paper forms part of the thesis work

of Westley Reeves presented in partial fulfillment of the degree of Doctor of Medicine, Yale University School of Medicine. Dr. Reeves was awarded the Dr. Harold Lamport Biomedical Research Prize for meritorious research completed during his medical training.

Received for publication 9 October 1979, and in revised form 15 February 1980.

REFERENCES

1. AINSWORTH, S. K., and M. J. KARNOVSKY. 1972. An ultrastructural staining method for enhancing the size and electron opacity of ferritin in thin sections. *J. Histochem. Cytochem.* **20**:225–229.
2. ANDERSON, H. C., and S. W. SAJDERA. 1971. The fine structure of bovine nasal cartilage. Extraction as a technique to study proteoglycans. *J. Cell Biol.* **49**:650–663.
3. ANDREWS, P. M. 1979. Glomerular epithelial alterations resulting from sialic surface coat removal. *Kidney Int.* **15**:376–385.
4. BERNFIELD, M. R., S. D. BANERJEE, and R. H. COHN. 1972. Dependence of salivary epithelial morphology and branching morphogenesis upon acid mucopolysaccharide-protein (proteoglycan) at the epithelial surface. *J. Cell Biol.* **52**:674–689.
5. BRENNER, B. M., C. BAYLIS, and W. M. DEEN. 1976. Transport of molecules across renal glomerular capillaries. *Physiol. Rev.* **56**:502–534.
6. BRENNER, B. M., T. H. HOSTETTER, and H. D. HUMES. 1978. Molecular basis of proteinuria of glomerular origin. *New Engl. J. Med.* **298**:826–833.
7. CAULFIELD, J. P., and M. G. FARQUHAR. 1974. The permeability of glomerular capillaries to graded dextrans. Identification of the basement membrane as the primary filtration barrier. *J. Cell Biol.* **63**:883–903.
8. CAULFIELD, J. P., and M. G. FARQUHAR. 1976. Distribution of anionic sites in glomerular basement membranes. Their possible role in filtration and attachment. *Proc. Natl. Acad. Sci. U. S. A.* **73**:1646–1650.
9. CLEMENTI, F., and G. E. PALADE. 1969. Intestinal capillaries. I. Permeability to peroxidase and ferritin. *J. Cell Biol.* **41**:33–58.
10. COHN, R. H., S. D. BANERJEE, and M. R. BERNFIELD. 1977. Basal lamina of embryonic salivary epithelia. Nature of glycosaminoglycan and organization of extracellular materials. *J. Cell Biol.* **73**:464–478.
11. DUBOIS, A. M. 1969. The embryonic kidney. *In* The Kidney: Morphology, Biochemistry, Physiology. Vol. I. C. Rouiller and A. F. Muller, editors. Academic Press, Inc., New York. 1–60.
12. FARQUHAR, M. G. 1978. Structure and function in glomerular capillaries. Role of the basement membrane in glomerular filtration. *In* Biology and Chemistry of Basement Membranes. N. A. Kefalides, editor. Academic Press, Inc., New York. 43–80.
13. FARQUHAR, M. G., and Y. S. KANWAR. 1979. Functional organization of the glomerulus: State of the science in 1979. *In* Immune Mechanisms in Renal Diseases. A. F. Michael and N. Cummings, editors. Academic Press, Inc., New York.
14. FARQUHAR, M. G., S. L. WISSIG, and G. E. PALADE. 1961. Glomerular permeability. I. Ferritin transfer across the normal glomerular capillary wall. *J. Exp. Med.* **113**:47–66.
15. HASCALL, V. C., and D. HEINEGARD. 1974. Aggregation of cartilage proteoglycans. II. Oligosaccharide competitors of the proteoglycan-hyaluronic acid interaction. *J. Biol. Chem.* **249**:4242–4249.
16. HAY, E. D., and S. MEIER. 1974. Glycosaminoglycan synthesis by embryonic inductors: neural tube, notochord, and lens. *J. Cell Biol.* **62**: 889–898.
17. HAY, E. D., D. L. HASTY, and K. L. KIEHNAU. 1978. C. Morphological investigation of fibers derived from various types. Fine structure of collagens and their relation to glucosaminoglycans (GAG). *In* Collagen-Platelet Interaction. H. Gastpar, K. Kühn, and R. Marx, editors. F. K. Schattauer Verlag, Stuttgart. 129–151.
18. HEINEGARD, D., and V. C. HASCALL. 1974. Aggregation of proteoglycans. III. Characteristics of the proteins isolated from trypsin digests of aggregates. *J. Biol. Chem.* **249**:4250–4256.
19. JONES, D. B. 1969. Mucosubstances of the glomerulus. *Lab. Invest.* **21**: 119–125.
20. KANWAR, Y. S., and M. G. FARQUHAR. 1979. Anionic sites in the glomerular basement membrane. In vivo and in vitro localization to the laminae rarae by cationic probes. *J. Cell Biol.* **81**:137–153.
21. KANWAR, Y. S., and M. G. FARQUHAR. 1979. Presence of heparan sulfate in the glomerular basement membrane. *Proc. Natl. Acad. Sci. U. S. A.* **76**:1303–1307.
22. KANWAR, Y. S., and M. G. FARQUHAR. 1979. Isolation of glycosaminoglycans (heparan sulfate) from the glomerular basement membrane. *Proc. Natl. Acad. Sci. U. S. A.* **76**:4493–4497.
23. KANWAR, Y. S., and M. G. FARQUHAR. 1980. Detachment of endothelium and epithelium from the glomerular basement membrane produced by kidney and perfusion with neuraminidase. *Lab. Invest.* **42**: 375–384.
24. KARNOVSKY, M. J. 1971. Use of ferrocyanide-reduced osmium tetroxide in electron microscopy. *In* Abstracts of the 11th Annual Meeting of the American Society of Cell Biology, New Orleans, La. 146.
25. KÜHN, K., and K. VON DER MARK. 1976. The influence of proteoglycans on the macromolecular structure of collagen. *In* Collagen-Platelet Interaction. H. Gastpar, K. Kühn, and R. Marx, editors. F. K. Schattauer Verlag, Stuttgart. 123–127.
26. LINDAHL, U., and M. HÖÖK. 1978. Glycosaminoglycans and their binding to biological macromolecules. *Annu. Rev. Biochem.* **47**:385–417.
27. LUFT, J. H. 1971. Ruthenium red and violet. II. Fine structural localization in animal tissues. *Anat. Rec.* **171**:369–416.
28. MANDL, I., J. D. MACLENNAN, and E. L. HOWES. 1953. Isolation and characterization of proteinase and collagenase from *Cl. histolyticum*. *J. Clin. Invest.* **32**:1323–1329.
29. MICHAEL, A. F., E. BLAU, and R. L. VERNIER. 1970. Glomerular polyanion. Alteration in aminonucleoside nephrosis. *Lab. Invest.* **23**: 649–657.
30. MOHOS, S. C., and L. SKOZA. 1969. Glomerular sialoprotein. *Science (Wash. D. C.).* **164**:1519–1521.
31. REEVES, W., J. P. CAULFIELD, and M. G. FARQUHAR. 1979. Differentiation of epithelial foot processes and filtration slits. Sequential appearance of occluding junctions, epithelial polyanion and slit membranes in developing glomeruli. *Lab. Invest.* **39**:80–100.
32. RENNKE, H. G., R. S. COTRAN, and M. A. VENKATACHALAM. 1975. Role of molecular charge in glomerular permeability. Tracer studies with cationized ferritins. *J. Cell Biol.* **67**:638–646.
33. RINEHART, J. F., and S. K. ABUL-HAJ. 1951. An improved method for histological demonstration of acid mucopolysaccharides in tissues. *A. M. A. Arch. Pathol.* **52**:189–194.
34. ROSENBERG, L., W. HELLMANN, and A. K. KLEINSCHMIDT. 1970. Macromolecular models of proteinpolysaccharides from bovine nasal cartilage based on electron microscopic studies. *J. Biol. Chem.* **245**:4123–4130.
35. SAITO, H., T. YAMAGATA, and S. SUZUKI. 1968. Enzymatic methods for the determination of small quantities of isomeric chondroitin sulfates. *J. Biol. Chem.* **243**:1536–1542.
36. SEILER, M. W., H. G. RENNKE, M. A. VENKATACHALAM, and R. S. COTRAN. 1977. Pathogenesis of polycation-induced alterations ("fusion") of glomerular epithelium. *Lab. Invest.* **36**:48–61.
37. SIMIONESCU, N., M. SIMIONESCU, and G. E. PALADE. 1979. Sulfate glycosaminoglycans are major components of the anionic sites of fenestrated diaphragms in capillary endothelium. *J. Cell Biol.* **83** (2, Pt. 2):78*a* (Abstr.).
38. SINGER, S. J. 1974. The molecular organization of membranes. *Annu. Rev. Biochem.* **43**:805–833.
39. TIMPL, R., G. WICK, and S. GAY. 1977. Antibodies to distinct types of collagens and procollagens and their application in immunohistology. *J. Immunol. Methods.* **18**:165–182.
40. THORNING, D., and R. VRACKO. 1977. Renal glomerular basal lamina scaffold. Embryologic development, anatomy, and role in cellular reconstruction of rat glomeruli injured by freezing and thawing. *Lab. Invest.* **37**:105–119.
41. TOOLE, B. P. 1976. Morphogenetic role of glycosaminoglycans (acid mucopolysaccharides) in brain and other tissues. *In* Neuronal Recognition. S. H. Barondes, editor. Plenum Publishing Corp., New York. 275–329.
42. TOOLE, B. P., and J. GROSS. 1971. The extracellular matrix of the regenerating newt limb: Synthesis and removal of hyaluronate prior to differentiation. *Dev. Biol.* **25**:57–77.
43. TOOLE, B. P., and R. L. TRELSTAD. 1971. Hyaluronate production and removal during corneal development in the chick. *Dev. Biol.* **26**:28–35.
44. TRELSTAD, R. L., K. HAYASHI, and B. P. TOOLE. 1974. Epithelial collagens and glycosaminoglycans in the embryonic cornea. Macromolecular order and morphogenesis in the basement membrane. *J. Cell Biol.* **62**:815–830.
45. VERNIER, R. L., and A. BIRCH-ANDERSON. 1962. Studies of the human fetal kidney. I. Development of the glomerulus. *J. Pediatr.* **60**:754–768.
46. VERNIER, R. L., and A. BIRCH-ANDERSON. 1963. Studies of the human fetal kidney. II. Permeability characteristics of the developing glomerulus. *J. Ultrastruct. Res.* **8**:66–88.
47. VERTEL, B. M., and A. DORFMAN. 1978. An immunohistochemical study of extracellular matrix formation during chondrogenesis. *Dev. Biol.* **62**:1–12.
48. WIGHT, T. N., and R. ROSS. 1975. Proteoglycans in primate arteries. I. Ultrastructural localization and distribution in the intima. *J. Cell Biol.* **67**:660–674.